The role of Ca^{2+} signaling in physiology and pathophysiology of the pancreatic ductal epithelial cells

Background

Human **pancreatic ductal epithelial** cells (PDEC) produce an alkaline fluid which is essential for normal digestion and crucially important for the maintaining the integrity of the pancreas. The function of pancreatic ductal fluid and HCO_3^- secretion plays a central role not just in the physiology, but also in the pathophysiology of the pancreas. **Impaired pancreatic fluid and HCO_3^- secretion can lead to pancreatic damage and to the development of acute pancreatitis** (AP), which is the most common reason for acute hospitalization among gastrointestinal disorder. Moreover, acut pancreatitis has an unacceptible high mortality and no specific treatment. Receptor induced intracellular Ca^{2+} release plays fundamental role in the regulation of HCO_3^- secretion, however **sustained intracellular Ca^{2+} elevations** in response to toxic factors inhibit secretory processes, cause mitochondrial damage and impaired ATP production leading the cell to necrosis. The pathological elevation of intracellular Ca^{2+} concentration ($[Ca^{2+}]_i$) is one of the hallmarks of the development of AP. Therefore, comprehensive analysis of the physiological and pathophysiological Ca^{2+} signalling of PDEC is crucially important since it may offer potential **therapeutic targets in AP**. So the aim of the study was to investigate the role of important elements of the Ca^{2+} signaling machinery (PMCA and TRPM2), which are responsible for **Ca^{2+} regulation, but their regulatory mechanisms are not fully understood in pancreatic ductal function**.

Results and discussion

1. TRPM2 channel and PMCA1 and 4 isoforms are expressed in the exocrine pancreas

First we wanted to confirm the presence of Transient Potential Melastatin-like 2 (TRPM2) and different plasma membrane Ca^{2+} ATPase (PMCA) isoforms on mRNA and protein level on pancreatic ductal cells. End-point PCR analysis of isolated ductal fragments confirmed that the TRPM2 gene was expressed in the exocrine pancreatic cells (Figure 1.A.). When immunofluorescent labelling of TRPM2 was performed on isolated acinar clusters and cross sections of isolated ducts, the confocal images showed that TRPM2 channels were expressed on the basolateral membrane of the pancreatic acinar cells, whereas an atypical expression pattern was seen in ductal cells (Figures 1.B–C).

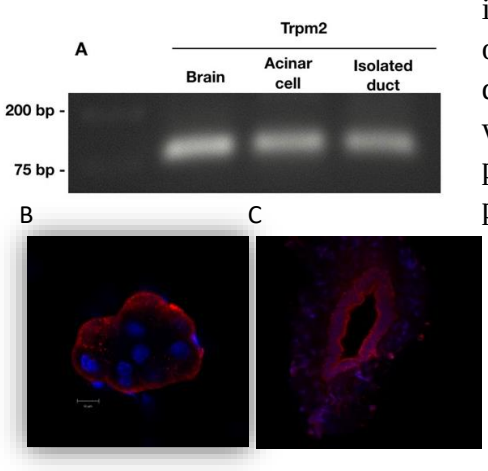

Figure 1. Expression of TRPM2 in the exocrine pancreas. A. Agarose gel images of cDNA samples derived from isolated acini and ductal fragments confirmed that the TRPM2 gene is expressed in the exocrine pancreas. **B–C.** Immunofluorescent labelling of TRPM2 on isolated acinar clusters and cross sections of isolated ducts. TRPM2 channels are expressed on the basolateral membrane of the pancreatic acinar cells and on the apical membrane in ductal cells. Scale bar: 10 μm

Reverse transcription polymerase chain reaction (RT-PCR) followed by endpoint analysis revealed strong expression of PMCA 1 and 4 both in whole pancreatic tissue and isolated

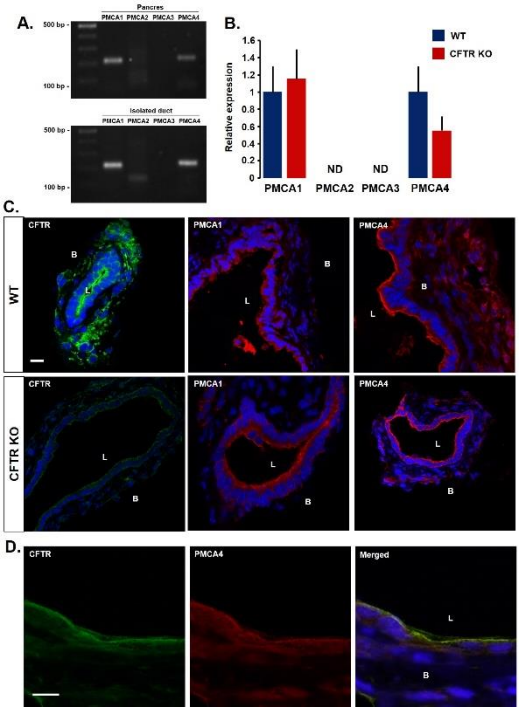

pancreatic ducts (Figure 2. A.). The PMCA2 gene showed low, but detectable expression in both samples. To compare the relative expression levels of PMCA genes we performed quantitative real-time PCR (qRT- PCR) in the isolated ductal fragments of WT and CFTR KO mice (Figure 2. B.), which showed no significant difference of PMCA1 and 4 expression in WT and CFTR KO mice. Next, we deciphered the expression of PMCA1 and 4 proteins in isolated pancreatic ducts with immunofluorescent labelling (Figure 2. C.). According to our results PMCA4 is expressed on the apical membrane of the pancreatic ductal epithelial cell, whereas PMCA1 showed an even distribution in the apical and basolateral membrane. The expression of PMCA1 and 4 was not altered in CFTR KO ducts, whereas a strong colocalization of PMCA4 and CFTR was visible at the apical membrane with a Mander's overlap coefficient of 0.906 (Figure 2. D.). These results suggest that the lack of CFTR expression diminishes the function of PMCA4 in ductal epithelial cells, rather than the expression.

Figure 2. The expression of PMCA isoforms in pancreatic ductal cells. A. Endpoint analysis of PMCA isoforms in whole pancreas (upper panel) and in isolated ducts (lower panel). The expression of PMCA1 and 4 was detected. **B.** Comparison of PMCA expression in WT and CFTR KO pancreatic ductal fragments with qRT- PCR showed no significant difference of PMCA1 and 4 expression. **C.** The expression of PMCA1 and 4 in isolated pancreatic ducts. PMCA4 is expressed on the apical membrane of the pancreatic ductal epithelia, whereas PMCA1 showed an even distribution in the plasma membrane. **D.** PMCA4 and CFTR colocalises at the apical membrane with a Mander's overlap coefficient of 0.906. Scale bars: 10 μm. B: basolateral side; L: lumen.

2. Functional TRPM2 channels are present in pancreatic ductal cells

Treatment of isolated WT pancreatic ductal fragments with 1 mM H_2O_2 induced a sustained elevation of $[Ca^{2+}]_I$ (Figure 3.C), which was significantly lower in TRPM2 KO ductal cells (0.30 ± 0.06 vs 0.10 ± 0.013, respectively). In these cells, Ca^{2+} elevation was significantly lower in Ca^{2+}-free conditions. Genetic inhibition of TRPM2 channels had no effect on the HCO_3^- secretion by pancreatic ductal cells (described below, Figures 3.). Therefore, the physiological relevance and function of TRPM2 in the exocrine pancreas still require further characterisation and study.

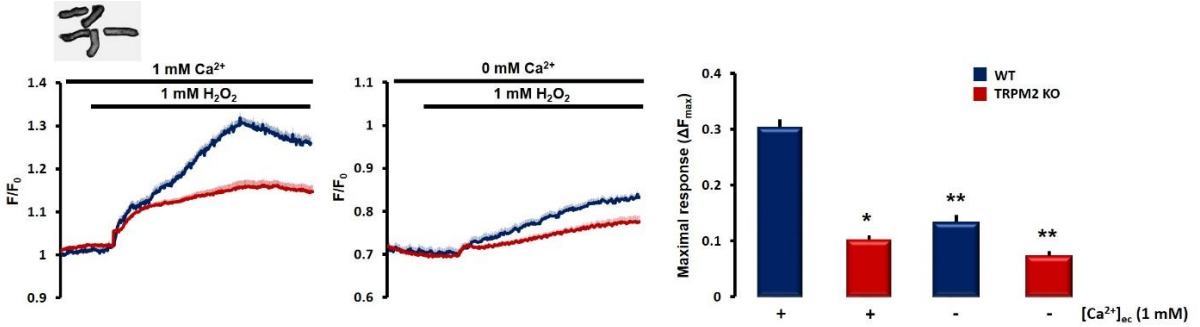

Figure 3. Functional activity of TRPM2 in pancreatic ductal fragments. Averages of intracellular Ca^{2+} recordings in isolated pancreatic ducts (5–6 experiments/group) in the presence or absence of extracellular Ca^{2+}. Bar charts summarise the maximal Ca^{2+} elevations evoked by H_2O_2, which was significantly lower in TRPM2 KO

ductal cells. These results suggest that TRPM2 mediates extracellular Ca^{2+} influx under an oxidative stress condition in pancreatic acinar and ductal cells. *: $p < 0.05$ vs WT.

3. TRPM2 contributes to bile-acid-induced extracellular Ca^{2+} influx in pancreatic acinar cells

Bile acids can cause the release Ca^{2+} from intracellular stores and can trigger extracellular Ca^{2+} influx. To study this, the intracellular Ca^{2+} elevation in response to bile acid treatment was compared in pancreatic acini and ducts. Administration of 250 µM chenodeoxycholate (CDC) was found to trigger a rapid, sustained increase in $[Ca^{2+}]_I$, which was markedly impaired in the TRPM2 KO acinar cells (0.834 ± 0.02 vs 0.655 ± 0.04) (Figure 3.A). These results highlight that TRPM2 plays an important role in bile-acid-induced extracellular Ca^{2+} influx in pancreatic acinar cells. By contrast, no significant difference was detected in isolated ductal fragments between the Ca^{2+} response of WT and TRPM2 KO ducts to 250 µM CDC, suggesting that, in ductal cells, TRPM2 plays no role in bile-acid-induced cell injury (Figure 3.B). Since HCO_3^- secretion is the primary function of the ductal epithelia, the HCO_3^- efflux across the apical membrane was compared between WT and TRPM2 KO ducts using fluorescent intracellular pH (pH_i) measurements [24]. Ductal cells were exposed to 20 mM NH_4Cl in HCO_3^-/CO_2-buffered solution from the basolateral membrane, triggering a rapid alkalisation because of the influx of NH_3 (Figure 3.C), followed by a slower recovery of the alkaline pH to the resting pH_i. This recovery phase depends on the HCO_3^- efflux (i.e. secretion) from the ductal epithelia via the SLC26 Cl^-/HCO_3^- exchangers and CFTR [24].

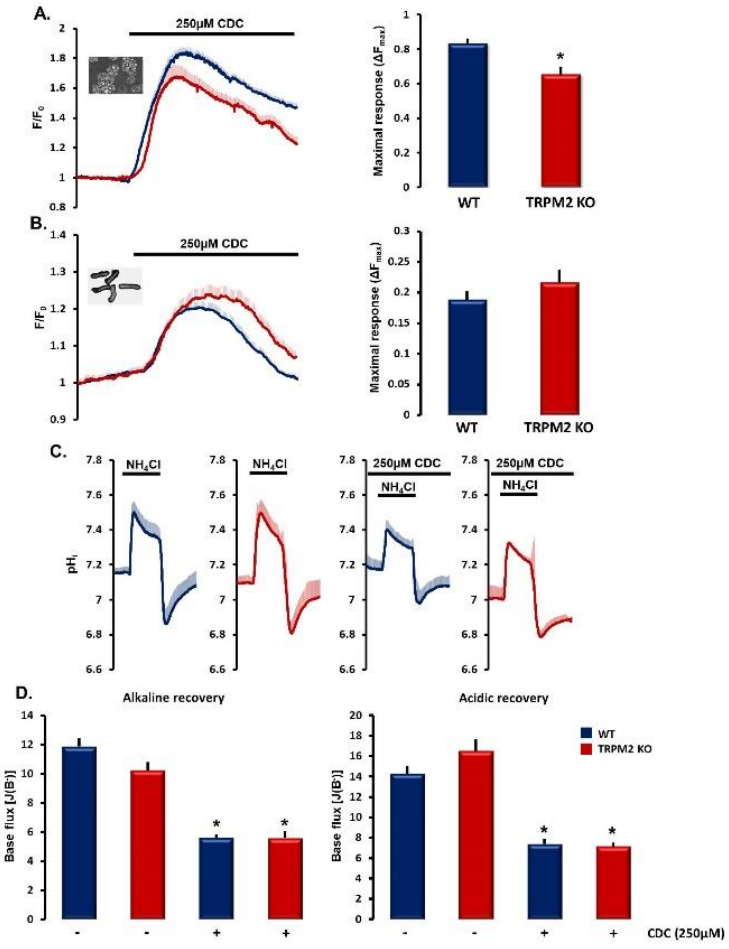

Figure 3. The role of TRPM2 in bile-acid-evoked Ca^{2+} signal generation. A–B. Average traces and bar charts of 5–6 individual experiments comparing intracellular Ca^{2+} elevations evoked by 250 µM CDC in WT and TRPM2 KO acini and isolated ducts. Genetic deletion of TRPM2 reduced the bile-acid-induced Ca^{2+} elevation in pancreatic acini, but not in ducts. *: $p < 0.05$ vs WT. **C.** Average pH_i traces of 4–6 experiments for each condition. Pancreatic ducts were perfused with HCO_3^-/CO_2-buffered extracellular solution, and intracellular alkalisation was achieved by 20 mM NH_4Cl administration. **D.** Bar charts of the calculated base fluxes of HCO_3^-. 250 µM CDC significantly decreased both alkaline and acidic recovery; however, no significant difference was detected in WT and TRPM2 KO ducts.

Removal of NH_4Cl rapidly decreased pH_i below the resting value, which is restored by the activities of the basolateral NHE1 and NBCe1 [24]. The initial recovery rates were measured (calculated as $\Delta pH/\Delta t$) over the first 30 s to calculate the base flux $[J(B^-)]$ values as described [24]. With this assay, no difference in the activities of the apical and basolateral proteins was found between WT and TRPM2 KO ducts (Figures 3.C–D). Although the administration of CDC markedly inhibited ion secretion as has been previously described

[12], the genetic knockout of TRPM2 demonstrated no protective effect, suggesting that bile acids affect ductal cells via a TRPM2-independent mechanism (Figures 3.C–D).

4. The function of plasma membrane Ca^{2+} pump is impaired in the absence of CFTR in pancreatic ductal cells

Cystic fibrosis transmembrane conductance regulator (CFTR) is expressed on the apical membrane of the pancreatic ductal epithelial cells in the exocrine pancreas and plays a fundamental role in the HCO_3^- secretion of pancreatic ductal cells. Therefore, first we wanted to compare the intracellular Ca^{2+} signalling in WT and CFTR KO pancreatic ductal cells. Therefore, to release the endoplasmic reticulum (ER) Ca^{2+} stores and trigger extracellular Ca^{2+} entry, we treated isolated ducts with 100 µM carbachol, which evoked a two-phase intracellular Ca^{2+} elevation both in WT and CFTR KO ductal cells (Figure 4. A.). The maximal Ca^{2+} release was not different, however we found that the slope of the plateau phase – representing the Ca^{2+} extrusion from the cytosol - was significantly increased in CFTR KO ducts compared to WT. To rule out that the observed difference is due to the non-specific tissue damage in CFTR KO mice we used isolated acinar cells, which don't express CFTR. We were not able to observe any difference in the maximal intracellular Ca^{2+} elevation, or in the slope of plateau phase upon carbachol treatment between acinar clusters of WT and CFTR KO mice (Figure 4. B.) suggesting that the alteration in ductal cells is due to the lack of CFTR function, or expression.

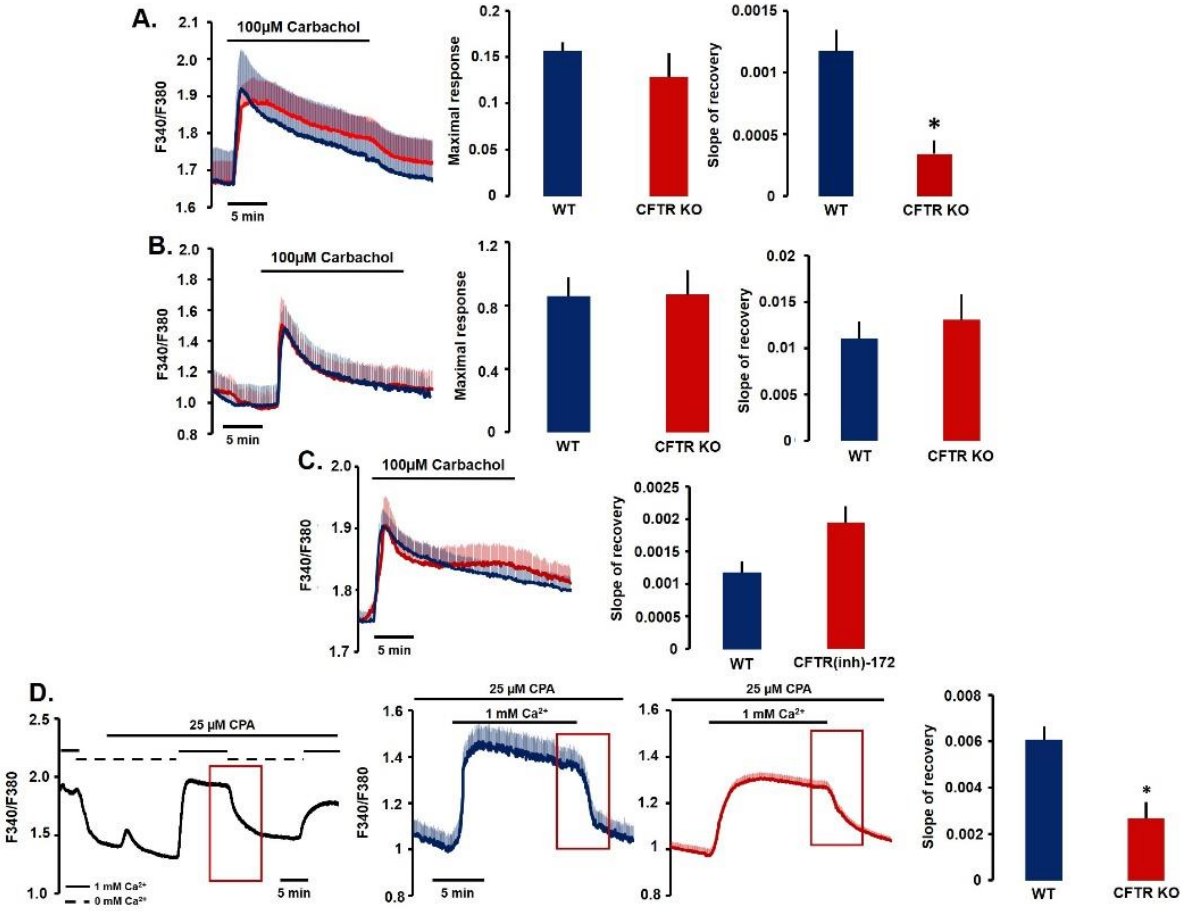

Figure 4. PMCA dysfunction in CFTR knockout pancreatic ductal cells. A. Average traces, maximal Ca^{2+} elevation and the slope of recovery in WT and CFTR KO pancreatic ductal fragments in response to 100 µM carbachol. The maximal Ca^{2+} release was not different, however Ca^{2+} extrusion was significantly impaired in CFTR KO ducts. **B.** Average traces, maximal Ca^{2+} elevation and the slope of recovery in WT and CFTR KO pancreatic acinar cells in response to 100 µM carbachol showed no difference. **C.** Average traces and the slope of

recovery demonstrates in WT pancreatic ductal fragments that inhibition of CFTR with 10 μM CFTR(inh)-172 has no effect on the response to carbachol. **D.** Complete ER Ca^{2+} store depletion was induced with 25μM cyclopoazonic-acid (CPA) in Ca^{2+}-free extracellular media. Re-addition of extracellular Ca^{2+} induced a SOCE-mediated rise in the intracellular Ca^{2+}, whereas Ca^{2+} extracellular removal trigger Ca^{2+} extrusion from the cytosol (red quadrant highlights the Ca^{2+} extrusion, which was used to calculate the slope of recovery). Under these conditions, the slope of Ca^{2+} efflux was significantly decreased in CFTR KO ductal cells. All averages were calculated from 6-10 individual experiments. *: $p< 0.05$ vs WT.

To clarify, whether the absence of CFTR function, or expression caused the alteration in the intracellular Ca^{2+} signalling we used a selective pharmacological inhibitor of CFTR. 10 μM CFTR(inh)-172 significantly impaired the regeneration of isolated ducts after alkali load, suggesting the inhibition of CFTR function. Notably, the carbachol-induced intracellular Ca^{2+} signalling was not different in 10 μM CFTR(inh)-172 treated WT ductal cells (Figure 4. C.) suggesting that the lack of CFTR function has no effect on the intracellular Ca^{2+} signalling. Next, we induced complete ER Ca^{2+} store depletion with 25μM cyclopoazonic-acid (CPA) in Ca^{2+}-free extracellular media. Under these conditions the store depletion activates the store operated Ca^{2+} influx (SOCE) and the re-addition of extracellular Ca^{2+} induces a SOCE-mediated rise in the intracellular Ca^{2+}. The inhibition of SERCA pump caused rapid release of the ER Ca^{2+} stores, which was not different in WT and CFTR KO cells (Figure 4. D). To evaluate Ca^{2+} extrusion we removed the extracellular Ca^{2+} again, which resulted in a rapid drop of intracellular Ca^{2+}. Under these conditions, the slope of Ca^{2+} efflux was significantly decreased in CFTR KO ductal cells. To avoid any potential errors in the evaluation, the slope of the Ca^{2+} extrusion was compared at the same intracellular Ca^{2+} levels. As Ca^{2+} extrusion in non-excitable cells can be mediated by the activity of PMCA and Na^{+}/Ca^{2+} exchanger (NCX), we used two inhibitors to rule out the contribution of NCX to Ca^{2+} extrusion. Neither the pan-NCX inhibitor CB-DMB nor SEA0400 had any effect, suggesting that NCX activity has no contribution to the Ca^{2+} efflux in ductal cells, and thus the activity of PMCA is impaired in CFTR KO ductal epithelial cells.

5. PMCA4 interacts with CFTR at the apical membrane of pancreatic ductal epithelial cells

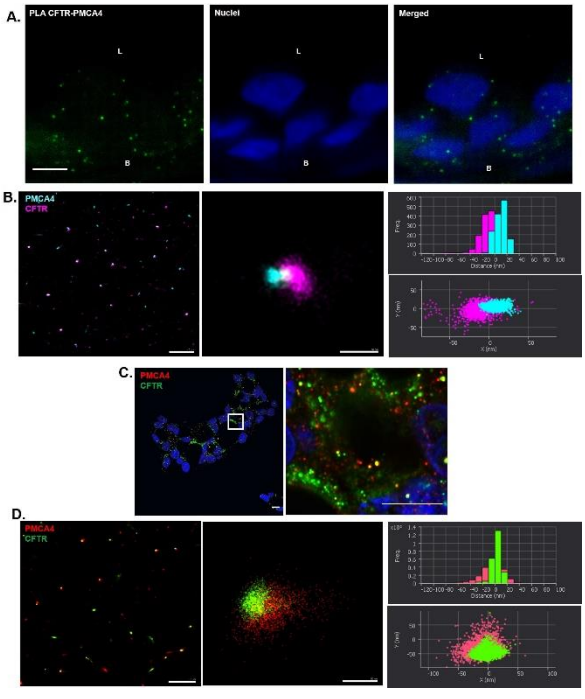

Our measurements suggested a close connection between CFTR and PMCA4, which seems to be required for the proper function of PMCA4 and for physiological Ca^{2+} extrusion. To characterize this connection further in cellular context Duolink proximity ligation assay (PLA) of endogenous PMCA and CFTR was performed. To avoid unspecific antibody binding, we used pancreatic ductal fragments isolated from guinea pig in this experiment. We confirmed that the expressions of PMCA4 and CFTR in guinea pig recapitulate the expression pattern of mice ductal cells. The Duolink PLA probe suggested that PMCA4 and CFTR are in a proximity of <40 nm (Figure 5. A.).

Figure 5. Interaction of PMCA4 with CFTR in pancreatic ductal epithelial cells. A. Duolink proximity ligation assay (PLA) of endogenous PMCA and CFTR was performed to assess the interaction of the two

proteins. For representation, 18 images of a Z-stack were merged. The PLA suggested that PMCA4 and CFTR are in a proximity of <40 nm. Scale bars: 10 μm. **B.** dSTORM images of Hela cells transfected with CFTR and PMCA4. This technique revealed a perfect overlap (<20 nm) between the two proteins in the plasma membrane. Scale bars: 1 μm and 50 nm respectively. **C.** Confocal images of 2D adherent primary ductal cells generated from human pancreatic ductal organoids. Scale bars: 5 μm. **D.** dSTORM images of CFTR and PMCA4 in primary human pancreatic ductal cells demonstrating a strong colocalization of native proteins. Scale bars: 1 μm and 50 nm respectively. n= 5-7 cells were analysed for each condition in dSTORM.

To be able to visualize this interaction with even higher resolution, we utilized the dSTORM technique first in Hela cells cotransfected with plasmids coding CFTR and PMCA4. This technique revealed a perfect overlap (<20 nm) between the two proteins in the plasma membrane suggesting a physical interaction between them (Figure 5. B). Next, we used 2D adherent primary human ductal cells generated from human pancreatic ductal organoids to confirm this interaction in endogenously expressed protein as well (Figure 5. C.). Similarly to Hela cells, the overlap of CFTR and PMCA4 was confirmed in primary human pancreatic ductal cells as well (Figure 5. D.).

6. Lack of TRPM2 decreases the severity of experimental biliary pancreatitis

After to characterization of TRPM2 in the physiological processes of pancreatic ducts, we start to determine the role of TRPM2 in the pathogenesis of AP. The disease severity of WT and TRPM2 KO animals was compared in two standard experimental AP models. In the first series of experiments, mice were given 10 hourly i.p. injections of either physiological saline (control group) or 50 μg/bwkg cerulein to induce AP (Figure 6.A). Overall, in this experimental model, no significant differences were detected between WT and TRPM2 KO mice. The control animals had normal pancreatic histology in both groups (Figure 6.A), whereas cerulein hyperstimulation caused extensive pancreatic damage. Despite this, no significant differences were observed in the histological parameters between the WT and TRPM2 KO animals. The extent of interstitial oedema (3.14 ± 0.25 for WT vs 3.03 ± 0.34 for KO), leukocyte infiltration (2.74 ± 0.53 for WT vs 3.04 ± 0.23 for KO, $p = 0.08$) or necrosis (18.64 ± 3.16 for WT vs 21.32 ± 3.58 for KO) was not found to be significantly different in the cerulein-treated groups (Figure 6.B).

More importantly, the role of the TRPM2 channel in the pathogenesis of biliary AP was also examined. In this model, pancreatitis was induced by intraductal infusion of 4% Na-taurocholate (TC) (control animals received physiological saline) as described previously. The infusion of 4% Na-taurocholate induced necrotising pancreatitis in both WT and TRPM2 KO mice, accompanied by elevated histological and laboratory parameters (Figures 6.C–D). The extent of interstitial oedema (2.8 ± 0.16 for WT vs 2.7 ± 0.2 for KO) or leukocyte infiltration (3.3 ± 0.38 for WT vs 2.7 ± 0.29 for KO, $p = 0.08$) was not significantly different in the Na-taurocholate-treated groups. Notably, the extent of necrosis was significantly higher in the WT group in comparison to the TRPM2 KO animals (41.3% ± 7.13% for WT vs 26.4% ± 5.5% for KO). In accordance with these findings, serum amylase activities were also significantly higher in the Na-taurocholate-treated WT animals versus the TRPM2 KO group. This perfectly mimicked the *in vitro* results obtained in this study, further confirming the crucial role of the TRPM2 channel in the pathogenesis of biliary AP.

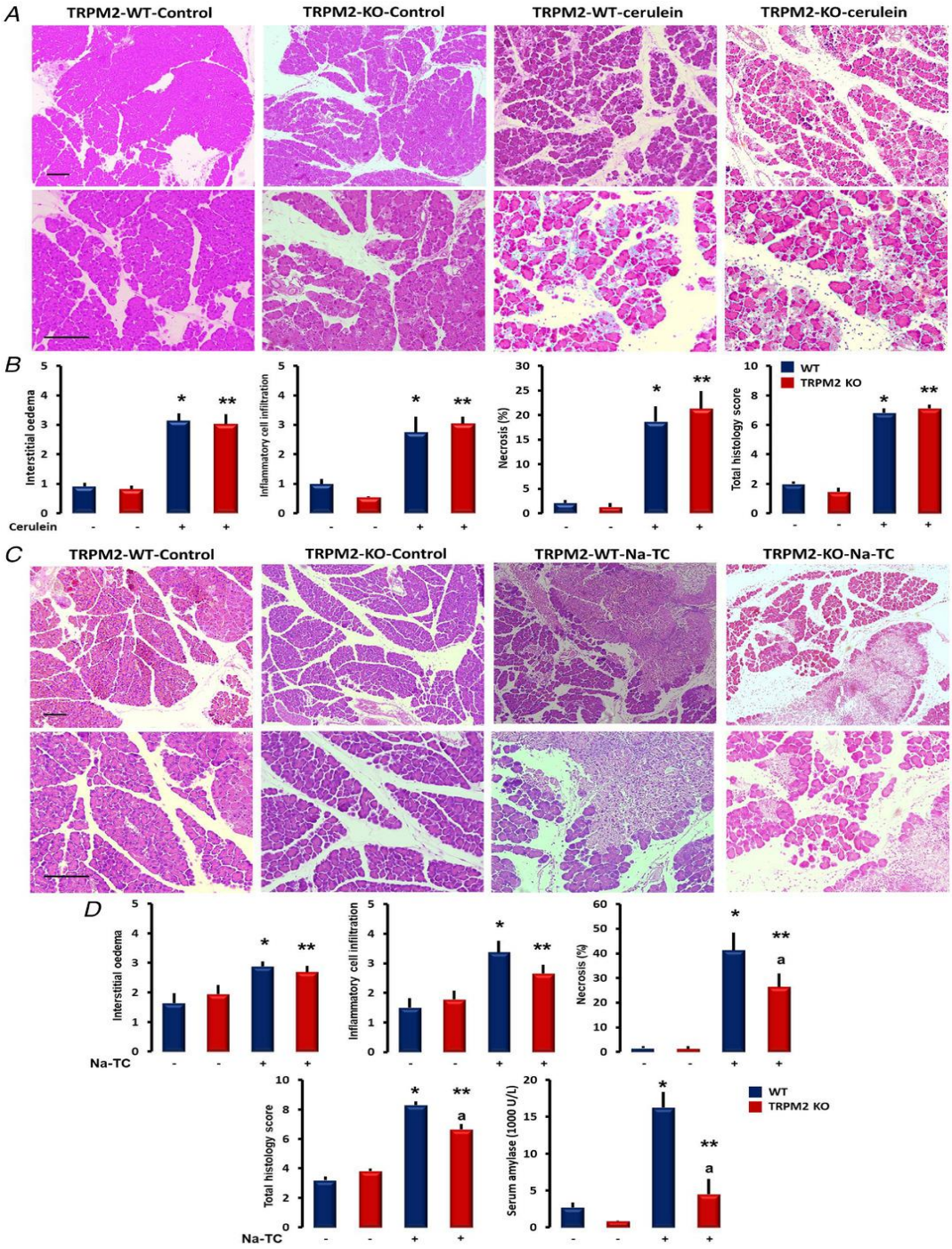

Figure 6. Genetic knockout of TRPM2 decreases the severity of biliary, but not cerulein-induced, acute pancreatitis. A. Representative images of pancreatic histology in cerulein-induced pancreatitis. Mice were given 10 hourly i.p. injections of either physiological saline (control group) or 50 μg/bwkg cerulein. **B.** Cerulein administration caused extensive pancreatic damage; however, no significant differences were observed in the histological parameters of WT and TRPM2 KO animals. n: 6–7 animals/groups; *: $p < 0.05$ vs WT; **: $p < 0.05$ vs TRPM2 KO. **C.** Representative images of pancreatic histology in Na-taurocholate-induced pancreatitis. Pancreatitis was induced by intraductal infusion of 4% Na-taurocholate (TC). **D.** The infusion of 4% Na-taurocholate-induced necrotising pancreatitis in WT and TRPM2 KO mice accompanied by elevated histological and laboratory parameters. Although the extent of interstitial oedema or leukocyte infiltration was not different, the extent of necrosis was significantly impaired in the TRPM2 KO animals. n: 6–7 animals/groups; *: $p < 0.05$ vs WT; **: $p < 0.05$ vs TRPM2 KO.

Taken together, we demonstrated that both pancreatic acinar and ductal cells express functionally active TRPM2, which can be activated by increased oxidative stress. Importantly, we also provided evidence that TRPM2 activity contributes to bile-acid-induced extracellular Ca^{2+} influx in acinar but not ductal cells, which increases the severity of bile-acid-induced experimental pancreatitis. These results suggest that inhibition of TRPM2 might be a potential option for use in treating biliary pancreatitis. On the other hand, we analysed for the first time the subcellular changes in the pancreatic ductal epithelia in CF and provided evidence that the intracellular Ca^{2+} homeostasis is disturbed by the decreased expression of CFTR channel in CF ductal cells. More specifically, using multiple independent model systems, we described the decreased activity of PMCA4, which colocalizes and physically interacts with CFTR on the apical membrane of the ductal cells. Based on these, the prevention of sustained intracellular Ca2+ overload may improve the exocrine pancreatic function in CF and may be a potential therapy to prevent CF-related AP episodes and the development of pancreatic diabetes.